

# Distinctive features gleaned from the comparative genomes analysis of clinical and non-clinical isolates of *Klebsiella pneumoniae*

Jina Rajkumari<sup>1</sup>, Supriyo Chakraborty<sup>2,\*</sup>, Piyush Pandey<sup>1,\*</sup>

<sup>1</sup>Department of Microbiology, Assam University, Silchar 788011, Assam, India; <sup>2</sup>Department of Biotechnology, Assam University, Silchar 788011, Assam, India; Piyush Pandey and Supriyo Chakraborty - Email: piyushddn@gmail.com, supriyoch\_2008@rediffmail.com; RKJ - Email: jinalantham.micro@gmail.com

Received January 29, 2020; Revised March 10, 2020, Accepted March 15, 2020; Published March 31, 2020

DOI: 10.6026/97320630016256

## Declaration on official E-mail:

The corresponding author declares that official e-mail from their institution is not available for all authors

## Declaration on Publication Ethics:

The authors state that they adhere with COPE guidelines on publishing ethics as described elsewhere at <https://publicationethics.org/>. The authors also undertake that they are not associated with any other third party (governmental or non-governmental agencies) linking with any form of unethical issues connecting to this publication. The authors also declare that they are not withholding any information that is misleading to the publisher in regard to this article.

## Abstract:

It is of interest to describe the distinctive features gleaned from the comparative genome analysis of clinical and non-clinical isolates of *Klebsiella pneumoniae*. The core genome of *K. pneumoniae* consisted of 3568 genes. Comparative genome analysis shows that *mdtABCD*, toxin-antitoxin systems are unique to clinical isolates and *catB*, *benA*, and transporter genes for citrate utilization are exclusive to non-clinical isolates. We further noted aromatic compound degrading genes in non-clinical isolates unlike in the later isolates. We grouped 88 core genes into 3 groups linked to infections, drug-resistance or xenobiotic metabolism using codon usage variation analysis. It is inferred using the neutrality plot analysis of GC12 with GC3 that codon usage variation is dominant over mutation pressure. Thus, we document data to distinguish clinical and non-clinical isolates of *K. pneumoniae* using comparative genomes analysis for understanding of genome diversity during speciation.

**Keywords:** *Klebsiella pneumoniae*, Comparative genomics, Codon usage bias

## Background

*Klebsiella pneumoniae* is a non-motile, gram-negative bacterium, which inhabits in diverse ecological niches ranging from soil to water and plants, and it is also opportunistic pathogen causing hospital-acquired disease in patients with the compromised

immune system [1]. Human clinical isolates are considered as indistinguishable from environmental isolates with respect to their biochemical reactions and other attributes [2]. In plants, *K. pneumoniae* strains had been reported to fix nitrogen and promote growth of the plants [3]. Rajkumari *et al.* [4] had reported that

*Klebsiella* strains have the ability to degrade hydrocarbons, including polyaromatic hydrocarbons (PAH). Previously, Holt et al. [5], have determined the diversity of genetic variation in specific genes associated with virulence and antibiotic resistance to track the emergence of invasive *K. pneumoniae* infections.

The advent of whole-genome sequencing along with reliable bioinformatics workflow has made possible to study the distinct genome patterns that may reflect the variation due to evolutionary pressures. Identification of conserved genomic core genes and pan genes from a collection of bacterial genomes depends on classifying orthologous genes based on similar sequences [6]. It provides valuable information and deeper insights into bacterial genome evolution, genes associated with host adaptation, virulence, and pathogenesis [7]. In previous work, the whole genome sequence analysis of clinical and environmental *K. pneumoniae* suggested that they are closely related but antibiotic resistance and virulence

factors were more frequent in clinical isolates. In fact, the phylogenomics analysis of *K. pneumoniae* whole genome failed to result in any distinct segregation of clinical and non-clinical clades of *K. pneumoniae*, as the genomes originating from either group were mixed throughout the tree [8].

Therefore, in this work, a genome analysis workflow was designed and used to identify the genes and their functions, which can be considered to resolve between clinical and non-clinical *K. pneumoniae* isolates (Figure 1). We used phylogenomics approach followed by the comparison of *K. pneumoniae* codon usage bias (CUB) pattern across the genes. In fact, the synonymous codons are known to be used non-randomly, and this unequal usage of the synonymous codon is called codon usage bias [9]. It is of interest to describe the distinctive features gleaned from the comparative genome analysis of clinical and non-clinical isolates of *K. pneumoniae*.

**Table 1:** Genomic features and comparison of *K. pneumoniae* genomes used for analysis

Strain	Size (bp)	CDS	GC (%)	Source	References
<i>K. pneumoniae</i> AWD5 (AWD5)	4807409	4636	58.18%	Non-clinical	Rajkumari et al. 2017
<i>K. pneumoniae</i> 342 (Kp342)	5641239	5768	56.87%	Non-clinical	Fouts et al. 2008
<i>K. pneumoniae</i> SKGH01 (SKGH01)	6088457	5777	56.54%	Clinical	Alfaresi 2018
<i>K. pneumoniae</i> subsp. <i>pneumonia</i> PittNDM01 (PNDM01)	5812304	5529	56.78%	Clinical	Doi et al. 2014
<i>K. pneumoniae</i> J1 (J1)	5406866	5039	57.24	Non-clinical	Pang et al. 2016
<i>K. pneumoniae</i> strain KCTC-2242 (KCT242)	5462423	5152	57.28	Non-clinical	Shin et al. 2012
<i>K. pneumoniae</i> subsp. <i>pneumonia</i> RJF293 (RJF293)	5450593	5077	57.20	Clinical	Wang et al. 2018
<i>K. pneumoniae</i> strain KP-1(KP-1)	5131085	4755	57.60	Non-clinical	Lee et al. 2013
<i>K. pneumoniae</i> NTUH-K2044 (NK2044)	5248520	5,006	57.7	Clinical	Wu et al. 2009
<i>K. pneumoniae</i> ATCC BAA- 2146 (BA2146)	5680367	5552	56.90	Clinical	Hudson et al. 2014
<i>K. pneumoniae</i> subsp. <i>pneumoniae</i> KPNIH10	5395263	5653	57.14	clinical	NZ_CP007727
<i>K. pneumoniae</i> subsp. <i>pneumoniae</i> KPNIH1	5394056	5654	57.14	clinical	NZ_CP008827
<i>K. pneumoniae</i> subsp. <i>pneumoniae</i> strain KPNIH33	5574202	5500	57.21	clinical	NZ_CP009771
<i>K. pneumoniae</i> subsp. <i>pneumoniae</i> KPNIH27	5241638	5932	56.71	clinical	NZ_CP007731
<i>K. pneumoniae</i> subsp. <i>pneumoniae</i> KPNIH24	536164	5590	57.12	clinical	NZ_CP008797
<i>K. pneumoniae</i> subsp. <i>pneumoniae</i> KPNIH30	5306618	5346	57.26	clinical	NZ_CP009872
<i>K. pneumoniae</i> strain XH209	5118878	4881	57.63	clinical	NZ_CP009461
<i>K. pneumoniae</i> strain CAV1016	5387681	5391	57.22	clinical	NZ_CP017934
<i>K. pneumoniae</i> strain CAV1042	5424949	5500	56.81	clinical	NZ_CP018671
<i>K. pneumoniae</i> strain CAV1596	5402147	5450	57.14	clinical	NZ_CP011647
<i>K. pneumoniae</i> strain CAV1417	5208900	5,373	56.98	clinical	NZ_CP018352
<i>K. pneumoniae</i> Kp_Goe_71070	5497083	5434	56.95	clinical	NZ_CP018450
<i>K. pneumoniae</i> Kp_Goe_827026	5373056	5662	56.62	clinical	NZ_CP018707
<i>K. pneumoniae</i> Kp_Goe_149473	5373056	5677	56.62	clinical	NZ_CP018686
<i>K. pneumoniae</i> Kp_Goe_152021	5373055	5673	56.62	clinical	NZ_CP018713
<i>K. pneumoniae</i> Kp_Goe_828304	5373056	5683	56.62	clinical	NZ_CP018719
<i>K. pneumoniae</i> MNCRE78	5454003	5584	56.86	clinical	NZ_CP018428
<i>K. pneumoniae</i> MNCRE53	5490693	5627	56.87	clinical	NZ_CP018437
<i>K. pneumoniae</i> Kp_Goe_154414	5159815	5618	56.62	clinical	NZ_CP018337
<i>K. pneumoniae</i> Kp_Goe_62629	5423372	5607	57.16	clinical	NZ_CP018364
<i>K. pneumoniae</i> Kp_Goe_33208	5497872	5429	56.96	clinical	NZ_CP018447
<i>K. pneumoniae</i> Kp_Goe_822917	5294741	5360	57.21	clinical	NZ_CP018438
<i>K. pneumoniae</i> strain CR14	5470889	5869	56.78	clinical	NZ_CP015392
<i>K. pneumoniae</i> Kp_Goe_121641	5478335	5390	56.96	clinical	NZ_CP018735
<i>K. pneumoniae</i> subsp. <i>pneumoniae</i> KPR0928	5309305	5286	57.32	clinical	NZ_CP008831
<i>K. pneumoniae</i> strain 34618	5313576	5487	57.21	clinical	NZ_CP010392
<i>K. pneumoniae</i> strain AR0049	5435743	5661	56.98	clinical	NZ_CP018816

*K. pneumoniae* strain K1

5453585

5237

57.44

clinical

NZ\_LOEJ01000001

## Methodology

### Genome comparison and Sequence Data

Comparative genome analysis of a collection of *K. pneumoniae* (clinical and non-clinical genomes) was examined. A private project was created with standard *K. pneumoniae* genomes, comprising of non-clinical/environmental and clinical isolates. Phylogenetic relationships between thirty-eight *K. pneumoniae* genomes were analyzed using EDGAR software platform (v.2.3) (<http://edgar.computational.bio>). EDGAR allows the calculation and identification of the core-pan genomes between different genomes. The nucleotide coding sequence (CDS) for eighty-eight genes, (24 drug resistant (DRGs), 16 infections related genes (IRGs) and 48 xenobiotic metabolism genes (XMGs) of five clinical and five non-clinical *K. pneumoniae* genomes having perfect start and stop codon were retrieved from IMG database (<http://img.jgi.doe.gov>) and gene details are given below.

### The effective number of codons

The observed effective number of codons (ENC) for each coding sequence of gene sets of *K. pneumoniae* was calculated using the formula given by Wright [10]. ENC value shows an inverse relationship with the degree of codon bias. ENC values range from 20 to 61, where low ENC value (<35) indicates high codon usage bias and high ENC value indicates low codon usage bias [10].

$$ENC = 2 + \frac{9}{F_2} + \frac{1}{F_3} + \frac{5}{F_4} + \frac{3}{F_6}$$

where  $F_k$  ( $k=2, 3, 4, 6$ ) is the mean of  $F_k$  values for the  $k$ -fold degenerate amino acids

### Nucleotide composition analysis

The overall nucleotide composition (A%, C%, T% and G%) and occurrence of overall frequency of the nucleotide (G+C) at first ( $GC_1$ ), second ( $GC_2$ ) and third ( $GC_3$ ) position of the synonymous codons were calculated in the coding sequences of the genes to quantify the extent of base compositional bias. The calculations were done using a Perl script developed by one of the authors (SC).

### Neutrality plot

The neutrality plot is a scattered plot, which is used to determine the role of directional mutational pressure against selection pressure during evolution. It is the regression of  $GC_{12}$  on  $GC_3$ , as the synonymous mutation occurs in the 3<sup>rd</sup> position of codon while non-synonymous mutations occur in the 1<sup>st</sup> and 2<sup>nd</sup> position. The non-synonymous mutation transforms the activity of the gene,

which resulted from the alteration of amino acid sequence. In neutrality plot, if the regression line falls near the diagonal, it signifies weak external selection pressure and the role of mutation pressure is dominant.

### Software and Statistical Analysis

Heat map of the specific clinical and non-clinical genes was generated by Expression Heatmapper using an average linkage method with Euclidean distance [11]. A network of genes was created for selected unique genes of clinical and non-clinical isolates by Cytoscape 3.4.0 with GeneMANIA plugin. The node degree distribution of the complex protein-protein interaction network was obtained from Cytoscape by Network analyzer [12]. A PERL program was developed to estimate the genetic codon usage bias indices and the selection pressure on the coding sequence of *K. pneumoniae* genes. Correlation analysis was performed to identify the degree of relationship between two parameters by Karl Pearson's method. The significance of the correlation coefficient was tested by t-test for (n-2) degrees of freedom at  $p < 0.01$  or  $p < 0.05$ . Statistical analyses were performed using IBM SPSS version 21.0 for windows.

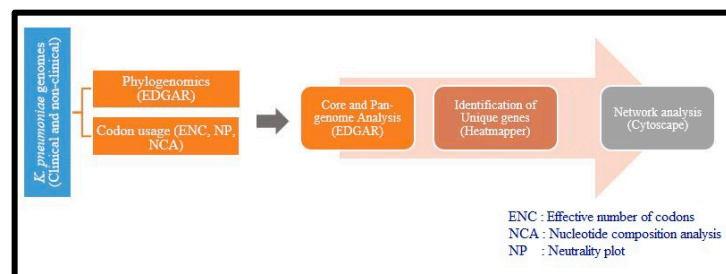
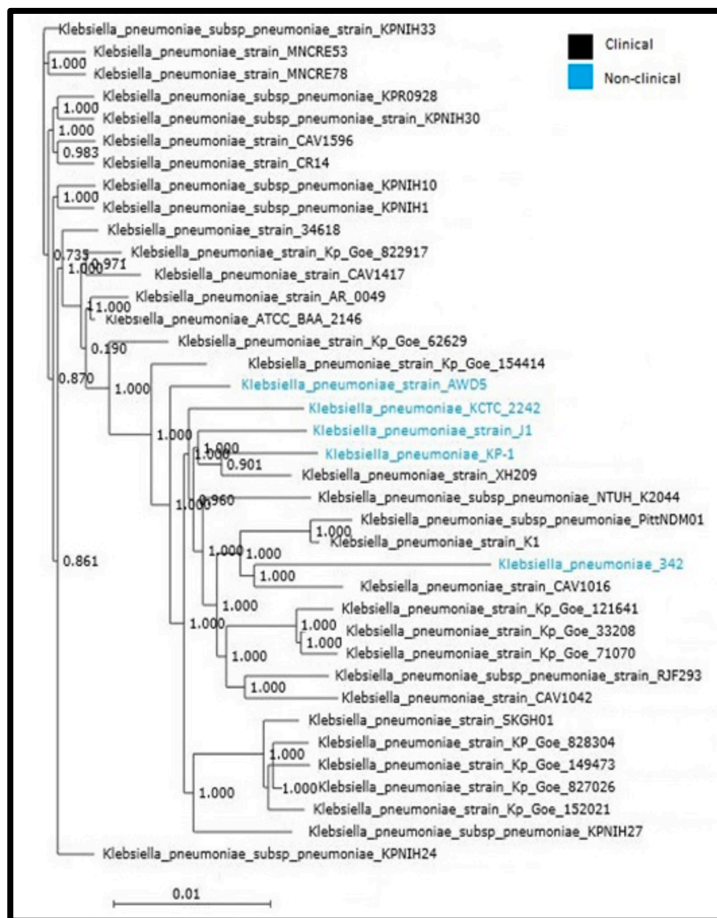


Figure 1: Flowchart of the workflow

### Results:

Phylogenomic relationship of *K. pneumoniae* (clinical and non-clinical) genomes was examined from the deduced amino acid sequences of the core genomes and resolved the close relationship among non-clinical and clinical isolates. The main features of the genome sequences of *K. pneumoniae* non-clinical strain and clinical strain are summarized below (Table 1). The tree was built out of core genome taking 3568 genes per genome, 135584 in total. There was no clear separation of clades between clinical and non-clinical isolates (Figure 2). Phylogenomic analysis of the core genomes 48 clinical and 29 environmental *K. pneumoniae* isolates had demonstrated that the isolates were intermixed and failed to result in any distinct segregation of clinical and non-clinical clades of *K. pneumoniae* [8].



**Figure 2:** Phylogenetic tree constructed from the core genome of *K. pneumoniae* genomes. The scale bar, 0.01 corresponds to the substitution per amino acid within the coding regions of the core genome.

Based on the phylogenomics results, genomes (clinical and non-clinical) were selected for further analysis and orthologous genes in *K. pneumoniae* were calculated. Core genome analyses of the *K. pneumoniae* genomes showed that it consisted of 3568 conserved genes. While the pan-genome appeared to grow rapidly and the core genome was limited to less than 4000 genes. There are several Pan-genome analysis pipelines are available [13, 14, 15, 16] however we have used EDGAR pipeline for studying genetic variation, and function enrichment analyses of the gene clusters. Core versus pan-genome development analysis of *K. pneumoniae* genomes revealed that 3568 formed the core genome while 11780 genes formed the

pan-genome when *K. pneumoniae* AWD5 is used as the reference genome (Figure 3). The genes in AWD5 strain cover 89.45% of the coding genes in the genome. Average nucleic acid identities (ANI) of AWD5 with *K. pneumoniae* KP-1, *K. pneumoniae* ATCC-BAA 2146 and *K. pneumoniae* subsp. *pneumoniae* NTUH-K2044 revealed 99% sequence homologies and 94.02% with *K. pneumoniae* 342. The genomes of AWD5 and ATCC BAA-2146 (clinical strain) appear to be most similar by sharing 4529 orthologs whereas 4442 orthologs were found between AWD5 and the environment isolate KP-1. Pan-genome of six *K. pneumoniae* strains was reported to be consisted of 4,829 core genes, such a high percentage signifies a high rate of conservation among the strains. Previously, some studies had reported that phenotypic and genetic features of *K. pneumoniae* of environmental and clinical origin were similar and therefore, the isolates cannot be distinguished [2, 17].

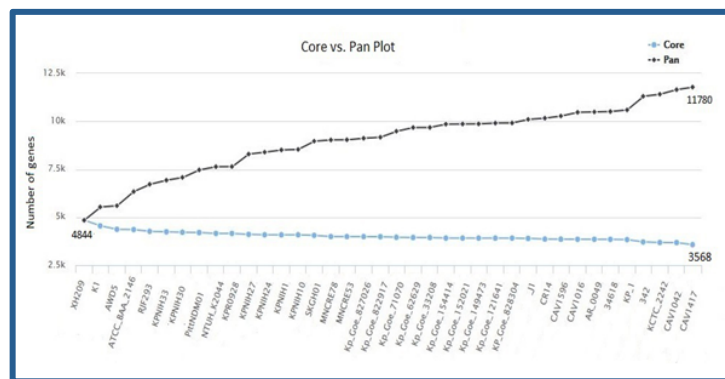


**Figure 3:** Core vs pan-genome development plot of *K. pneumoniae* genomes (EDGAR 2.2 software platform)

### Gene content analysis of *K. pneumoniae*

By investigating the presence and absence of genes in *K. pneumoniae*, most of the regions within the genomes were found to be conserved, including the virulence genes present in the clinical strains regardless of disease source. The orthologs include components of regulatory pathways such as basic transcriptional machinery, DNA replication, homologous recombination, mismatch repair, nucleotide excision repair, bacterial secretion system and protein export. Genes attributable to the production of indole-3-acetic acid (IAA) (*ipdC*), solubilization of phosphate (*pqqABCDEF*, *phn* and *pho* gene clusters, *pstBACS*), synthesis of siderophore (*ent*, *fep* gene clusters), acetoin and 2,3-butanediol (*alsDSR*, *budC*) are found to be conserved. It also revealed the presence of multicomponent nitrate or nitrite transport system. More than 13 genes involved in benzoate (*ben* genes), catechol (*cat* genes),

protocatechuate (*pca* genes) were conserved in the core genome of *K. pneumoniae*.

Further, to obtain the unique genes, the genomes were segregated into two groups i.e., clinical and non-clinical, taking five genomes for each group and analyzed separately. In clinical isolates, such core genes included virulence factor capsule assembly protein, multidrug transporter subunit (*mdtABCD*), type II toxin-antitoxin systems, and type VI secretion system (TVISS). TVISS were found to be shared among clinical and non-clinical isolates however, at least eight CDSs determined in clinical genomes involved in TVISS, were not found in non-clinical isolates. It has been reported that an environmental isolate Kp342 and clinical isolate MGH78578 seemed to share core components of TVISS [18]. The unique core genome of non-clinical isolate consisted of aromatic compound degrading genes *catB*, *benA* and several transporters including genes for citrate utilization. This was in agreement to the hypothesis that environmental isolates are more versatile for their catabolic processes, as the ability to degrade organic compounds govern the evolution of novel catabolic abilities of bacteria that can survive in different habitats [19]. We took the presence/absence of such individual genes as the categorical analyst parameter subjected to build a phylogenetic tree. And showed that the strains from similar clinical and environmental sources were not linked than those from different sources (Figure 4). The core genes discriminated the clinical and environmental genomes and accessory genes segregated the strains within the group. Based on the gene functions, several gene sets were experimented which may resolve clinical and non-clinical isolates. Accordingly, one set of unique core genes in non-clinical isolates and clinical isolates is given in the figure 4 on the basis of which genomes were resolved into two distinct categories, further few genes were useful for resolving the genomes within the particular group. Virulence factor (*galF*, *wcaI*, *wcaG*, *wzb*, *wzc*, *manBC*), allantoin utilization genes (*gcl*, *allABCDS*, *ybbW*), TVISS (*impL*, *vgrG*, *tssFGJ*) and other antibiotic resistance genes were also observed as accessory genes in ten *K. pneumoniae*. The clinical genomes possessed multidrug resistance gene *bla<sub>CTX-M-15</sub>* as accessory gene; this is an indication of horizontal gene transfer that might have occurred between virulent and multidrug-resistant *K. pneumoniae* strains [20]. This finding agrees with the previous study, which reported that resistance to multiple antibiotics was found to be more frequent in clinical origin than that of environmental origin [21]. The gene interaction network of specific core genes of clinical and non-clinical *K. pneumoniae* genomes was analyzed in cytoscape and GeneMANIA (Figure 5) and data is given in supplementary file. It was noted that the functional partners were not part of the core genome of the respective group;

however, it surely had interactions, and hence influence the functions of these genes.

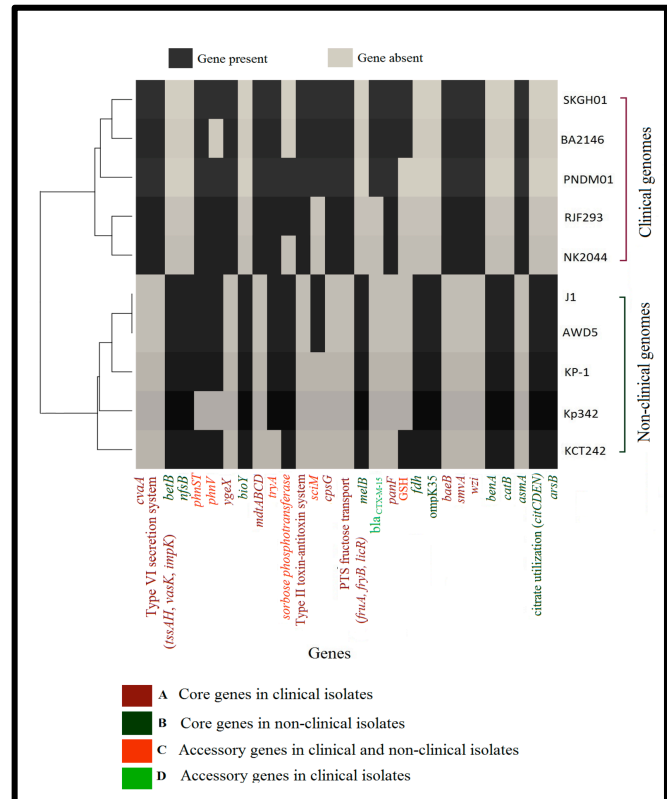


**Figure 4:** Dendrogram showing the relationship between genomes based on the presence and absence of genes designated as group specific.

### Extent of Codon usage variation in *K. pneumoniae*

In order to analyze codon usage variation five *K. pneumoniae* genomes were selected considering their level of similarity. The data set was restricted to 5 genomes to avoid non-ambiguity. According to the EDGAR interface, genes were placed at intersections of the Venn diagram only if they were reciprocal matches. The analysis utilizes all CDS of the genomes and it is not restricted to the core genome. Among the *K. pneumoniae* strains, AWD5 chromosome shared 31 orthologous CDS with BA2146 and further 188 CDS conjointly with the strain KP-1. Moreover, 65 orthologous CDS are found to be shared conjointly by environmental isolates AWD5, KP-1 and Kp342 (Figure 6). Also, it indicated that AWD5 has 10 singleton genes. Besides, the singletons that resemble to the genes without reciprocal best hit to another



The codon usage variation was studied for eighty-eight genes (24 DRGs, 16 IRGs, and 48 XMGs) from five *K. pneumoniae* genomes of non-clinical origin (Kp342, KP-1, AWD5) and clinical origin (NK2044, BA2146) core genome. Selected genes details are given in the supplementary file (**Table 2**).

To quantify the extent of variation in codon usage among different genomes of *K. pneumoniae*, the effective number of codon (ENC) values for three gene sets of each genome was calculated. The ENC is a non-directional measure of codon usage bias, widely used to measure for individual genes. The ENC values among five *K. pneumoniae* strains ranged from 37.1 to 39.71, indicating low codon usage bias (**Table 3**) for IRGs, DRGs and XMGs respectively. (ENC

< 40) represents stable ENC values and indicates that there is almost no variation of codon usage bias among the genes of *K. pneumoniae*. It also indicates conserved genomic composition among different *K. pneumoniae* genomes. Correlation analysis between codon usage bias and compositional properties of GC content were analyzed to understand the effect of base composition on codon usage bias. Negative correlation was observed between ENC and GC composition (**Table 4**). These results suggested that natural selection might have played an important role in codon usage pattern across the genes. Our results show that codon usage bias and gene expression among different *K. pneumoniae* genomes was lower, slightly biased in the genes [22].

**Table 2: Selected gene of *K. pneumoniae* and functions**

Sl.no	Gene	Protein function
1	<i>lepA</i>	GTP-binding protein
2	<i>ureC</i>	urease subunit alpha
3	<i>groL</i>	chaperonin GroEL
4	<i>fimA</i>	type 1 major fimbrial subunit precursor
5	<i>fimD</i>	putative export and assembly usher protein of type 1 fimbriae
6	<i>fimG</i>	type 1 fimbrial minor component
7	<i>fimH</i>	type 1 fimbrial adhesin precursor
8	<i>cyaA</i>	adenylate cyclase
9	<i>sdhA</i>	succinate dehydrogenase subunit A
10	<i>tolC</i>	outer membrane channel protein
11	<i>norW</i>	nitric oxide reductase
12	<i>norV</i>	anaerobic nitric oxide reductase flavorubredoxin
13	<i>RpoS</i>	RNA polymerase, sigma 38 subunit
14	<i>RpoN/SigL</i>	RNA polymerase, sigma 54 subunit
15	<i>yegQ</i>	putative protease
16	<i>LuxS</i>	S-ribosylhomocysteine lyase/quorum-sensing autoinducer 2 (AI-2) synthesis protein
17	<i>arnA</i>	UDP-4-amino-4-deoxy-L-arabinose formyltransferase
18	<i>arnB</i>	UDP-4-amino-4-deoxy-L-arabinose-oxoglutarate aminotransferase
19	<i>arnC</i>	undecaprenyl-phosphate 4-deoxy-4-formamido-L-arabinose transferase
20	<i>arnF</i>	undecaprenyl phosphate-alpha-L-ara4N flippase subunit
21	<i>arnT</i>	4-amino-4-deoxy-L-arabinose transferase
22	<i>amiA</i>	N-acetylmuramoyl-L-alanine amidase
23	<i>amiB</i>	N-acetylmuramoyl-L-alanine amidase
24	<i>sapB</i>	cationic peptide transport system permease protein
25	<i>sapC</i>	cationic peptide transport system permease protein
26	<i>sapD</i>	cationic peptide transport system ATP-binding protein
27	<i>sapF</i>	cationic peptide transport system ATP-binding protein
28	<i>basS</i>	two-component system, OmpR family, sensor histidine kinase
29	<i>mraY</i>	Phospho-N-acetylmuramoyl-pentapeptide-transferase
30	<i>oppA</i>	oligopeptide transport system substrate-binding protein
31	<i>oppB</i>	oligopeptide transport system permease protein
32	<i>oppC</i>	oligopeptide transport system permease protein
33	<i>oppD</i>	oligopeptide transport system ATP-binding protein
34	<i>oppF</i>	oligopeptide transport system ATP-binding protein
35	<i>ppiA</i>	peptidyl-prolyl cis-trans isomerase A (cyclophilin A)
36	<i>phoP</i>	two-component system, OmpR family, response regulator
37	<i>phoQ</i>	two-component system, OmpR family, sensor histidine kinase
38	<i>ftsI</i>	peptidoglycan synthetase
39	<i>dnaK</i>	molecular chaperone
40	<i>marA</i>	transcriptional regulator, AraC family
41	<i>benA/xylX</i>	benzoate/toluate 1,2-dioxygenase alpha subunit,

42	<i>catA</i>	catechol 1,2-dioxygenase
43	<i>catB</i>	muconate cycloisomerase
44	<i>catC</i>	muconolactone D-isomerase
45	<i>pcaB</i>	3-carboxy-cis,cis-muconate cycloisomerase,
46	<i>pcaD</i>	3-oxoadipate enol-lactonase
47	<i>pcaG</i>	protocatechuate 3,4-dioxygenase alpha subunit,
48	<i>pcaH</i>	protocatechuate 3,4-dioxygenase beta subunit,
49	<i>pcaI</i>	3-oxoadipate CoA-transferase alpha subunit,
50	<i>pcaJ</i>	3-oxoadipate CoA-transferase beta subunit,
51	<i>paaA</i>	ring-1,2-phenylacetyl-CoA epoxidase subunit,
52	<i>paaF</i>	enoyl-CoA hydratase
53	<i>paaH</i>	3-hydroxybutyryl-CoA dehydrogenase,
54	<i>paaK</i>	phenylacetate-CoA ligase
55	<i>paaZ</i>	oxepin-CoA hydrolase / 3-oxo-5,6-dehydrosuberil-CoA semialdehyde dehydrogenase,
56	<i>gabD</i>	succinate semialdehyde dehydrogenase,
57	<i>gabT</i>	4-aminobutyrate aminotransferase / (S)-3-amino-2-methylpropionate transaminase,
58	<i>glnB</i>	nitrogen regulatory protein P-II family,
59	<i>Gst</i>	glutathione S-transferase
60	<i>hpaA</i>	AraC family transcriptional regulator, 4-hydroxyphenylacetate 3-monooxygenase operon regulatory protein,
61	<i>hpaC</i>	4-hydroxyphenylacetate 3-monooxygenase reductase component,
62	<i>hpaD/hpcB</i>	3,4-dihydroxyphenylacetate 2,3-dioxygenase,
63	<i>hpaF</i>	5-carboxymethyl-2-hydroxymuconate delta isomerase,
64	<i>hpaH</i>	2-oxohept-3-enedioate hydratase,
65	<i>hpaG</i>	5-carboxy-2-oxohept-3-enedioate decarboxylase HpaG1 subunit
66	<i>hpaG</i>	5-carboxy-2-oxohept-3-enedioate decarboxylase HpaG2 subunit
67	<i>mhpA</i>	3-hydroxyphenylpropionate hydroxylase,
68	<i>mhpB</i>	2,3-dihydroxyphenylpropionate 1,2-dioxygenase,
69	<i>mhpC</i>	2-hydroxy-6-ketono-2,4-dienedioate hydrolase,
70	<i>mhpD</i>	2-keto-4-pentenoate hydratase
71	<i>mhpE</i>	4-hydroxy 2-oxovalerate aldolase
72	<i>mhpF</i>	acetaldehyde dehydrogenase
73	<i>entA</i>	2,3-dihydro-2,3-dihydroxybenzoate dehydrogenase,
74	<i>entB</i>	bifunctional isochorismate lyase / aryl carrier protein,
75	<i>entC</i>	isochorismate synthase
76	<i>entD</i>	enterobactin synthetase component D,
77	<i>fepA</i>	outer membrane receptor for ferrienterochelin and colicins,
78	<i>fepB</i>	iron complex transport system substrate-binding protein,
79	<i>fepC</i>	iron complex transport system ATP-binding protein,
80	<i>fepD</i>	iron complex transport system permease protein,
81	<i>pqqB</i>	pyrroloquinoline quinone biosynthesis protein B,
82	<i>pqqC</i>	pyrroloquinoline-quinone synthase,
83	<i>pqqD</i>	pyrroloquinoline quinone biosynthesis protein D,
84	<i>pqqE</i>	pyrroloquinoline quinone biosynthesis protein E,
85	<i>pstA</i>	phosphate ABC transporter membrane protein 2, PhoT family,
86	<i>pstB</i>	phosphate ABC transporter ATP-binding protein, PhoT family,
87	<i>pstC</i>	phosphate ABC transporter membrane protein 1, PhoT family,
88	<i>pstS</i>	phosphate ABC transporter substrate-binding protein, PhoT family,

**Table 3:** Nucleotide composition analysis in the coding sequence of gene sets in *K. pneumoniae* strains

Sl. No.	A	T	G	C	AT%	GC%	GC1%	GC2%	GC3%	AT3%	GC12%	ENC
<b>Infection-related gene</b>												
AWD5	313.1	259.9	403.8	435.6	40.7	59.3	63.4	42.3	72.1	27.9	52.8	38.19
KP-1	308.8	260.9	406.6	431.2	40.5	59.5	63.8	42.5	72.1	27.8	52.8	38.46
Kp342	299.7	247.1	385.8	415.4	40.6	59.5	63.9	42.2	72.2	27.8	53.1	37.56
BA2146	296.3	248.1	386.2	411.3	41	59	63.8	41.7	71.4	28.6	52.9	39.21
NK2044	297.2	248.8	390.1	415.4	40.5	59.5	63.8	42.5	72.2	27.7	53.2	38.64
Mean	303.02	252.96	394.5	421.78	40.66	59.36	63.74	42.24	72	27.96	52.96	38.91
SD	7.501	6.827	9.96	10.85	0.207	0.219	0.195	0.328	0.339	0.365	0.182	0.61
<b>Drug resistance gene</b>												
AWD5	214.8	210.8	302.3	323.2	40.4	59.5	64.4	40.6	73.5	26.4	52.6	39.23

KP-1	213.4	211	302.5	321.2	40.5	59.5	64.5	40.7	73.3	26.6	62.9	39.17
Kp342	220.5	218.2	310	325.5	40.7	59.3	64.3	40.9	72.6	27.3	62.6	39.71
BA2146	214.9	212.9	301.6	319.7	40.6	59.3	64.3	40.8	72.9	27.1	62.7	39.5
NK2044	213.9	211	303.4	322.1	40.3	59.6	64.6	40.7	73.5	26.5	63.1	39.3
Mean	215.5	212.78	303.96	322.34	40.5	59.44	64.42	40.74	73.16	26.78	60.78	39.38
Xenobiotic metabolism gene												
SD	2.864	3.148	3.437	2.182	0.158	0.134	0.131	0.114	0.397	0.396	4.577	0.22
AWD5	183.5	168.7	285.3	296.6	38.3	61.7	67.1	43.4	74.6	25.3	55.3	38.93
KP-1	178.2	161.3	271.7	285.7	38.3	61.7	67.1	43.5	74.5	25.4	55.3	39.1
Kp342	179.1	162.8	270.6	284.2	38.5	61.5	66.9	43.5	73.8	26.1	55.2	39.36
BA2146	178.3	160.8	271.6	285.3	38.3	61.7	67.1	43.5	74.5	25.5	55.2	37.1
NK2044	177.8	160.6	271.3	284.8	38.3	61.7	67.1	43.4	74.4	25.6	55.3	38.19
Mean	179.38	162.84	274.1	287.32	38.34	61.66	67.06	43.46	74.36	25.58	55.26	38.52
SD	2.351	3.387	6.276	5.218	0.089	0.089	0.089	0.055	0.321	0.311	0.054	0.91

SD: standard deviation, GC12: the average of GC contents at first and second codon positions.

**Table 4:** Summary of correlation analysis between ENC and various GC content

ENC	GC	GC1	GC2	GC3
AWD5 r	-0.414*	-0.443*	-0.184	-0.245
p value	0.044	0.03	0.388	0.249
KP-1 r	-0.440*	-0.440*	-0.212	-0.265
p value	0.031	0.032	0.319	0.211
KP342 r	-0.386	-0.511**	0.148	-0.298
p value	0.057	0.009	0.481	0.148
BA2146 r	-0.466*	-0.474*	-0.079	-0.356
p value	0.022	0.019	0.715	0.087
NK2044 r	-0.441*	-0.450*	-0.228	-0.265
p value	0.031	0.027	0.284	0.211

ENC	GC	GC1	GC2	GC3
AWD5 r	-0.275	-0.426	0.206	-0.155
p value	0.302	0.1	0.444	0.566
KP-1 r	0.047	-0.312	0.311	0.017
p value	0.863	0.239	0.24	0.949
KP342 r	0.042	-0.208	0.014	0.184
p value	0.877	0.439	0.958	0.496
BA2146 r	-0.527*	-0.520*	0.127	-0.437
p value	0.036	0.039	0.639	0.091
NK2044 r	-0.028	-0.359	0.32	-0.063
p value	0.918	0.171	0.227	0.817

ENC	GC	GC1	GC2	GC3
AWD5 r	-0.348*	0.026	-0.22	-0.503**
p value	0.015	0.86	0.133	0
KP-1 r	-0.369**	-0.01	-0.194	-0.516**
p value	0.01	0.947	0.186	0
KP342 r	-0.384**	0.056	-0.203	-0.580**
p value	0.007	0.708	0.167	0
BA2146 r	-0.395**	-0.018	-0.272	-0.520**
p value	0.005	0.902	0.061	0
NK2044 r	-0.339*	0.03	-0.243	-0.475**
p value	0.019	0.839	0.096	0.001

\*P < 0.05, \*\*P < 0.001

Nucleotide composition analyses of coding sequences of IRGs, DRGs, and XMGs (Table 3) showed mean percentage of GC and AT compositions was 59.44% and 40.5% in IRGs, 59.36% and 40.66% in

DRGs and 61.66% and 38.34% in XMGs respectively. Genes were GC-rich, GC content at the third position was higher than at the first and second codon position and the greatest difference of GC content was found between the second and the third codon positions. Hence, the overall nucleotide composition suggested that the nucleotide C and G occurred more frequently compared to A and T in the coding sequences and it is expected that G/C-ended codons might be preferred over A/T ended codons in the genomes. The difference in frequencies of A and T and to that of G and C were not the same which indicates that natural selection might have played a role in codon usage pattern [22].

**Table 5:** Summary of correlation analysis of GC12 Vs GC3

	GC12	AWD5 GC3	KP-1 GC3	Kp342 GC3	BA2146 GC3	NK2044 GC3
Drug resistance gene	r	0.478*	0.454*	0.305	0.440*	0.429*
	p	0.018	.026	0.138	0.031	0.037
Infection related gene	r	0.038	-0.069	-0.009	0.222	-0.026
	p	0.888	0.800	0.974	0.408	0.923
Xenobiotic metabolism gene	r	0.478**	0.482**	0.483**	0.499**	0.503**
	p	0.001	0.001	0.001	0.000	0.000

\*P < 0.05, \*\*P < 0.001

A neutrality plot analysis of GC12 (average value of GC1 and GC2) versus GC3 (Figure 7) was drawn to characterize the correlation of the three codon position of GC [23], and to estimate the influence of selection and mutation pressure on codon usage bias of IRGs, DRGs and XMGs of five *K. pneumoniae* strains [24]. The regression coefficient of GC12 on GC3 for IRGs of the *K. pneumoniae* strains AWD5, BA2146, KP-1, Kp342 and NK2044 were 0.0133, 0.0701, 0.0249, 0.0033 and 0.0099 indicating relative neutrality of 1.33%, 7.01%, 2.49%, 0.33%, and 0.99% respectively. The GC12 was influenced by mutation pressure and natural selection with a ratio of 1.33/98.67=0.014, 7.01/92.99=0.075, 2.49/97.51=0.026, 0.33/99.67=0.003, and 0.99/99.01=0.009 for AWD5, BA2146, KP-1, Kp342 and NK2044 respectively. The subsequent correlation

analysis revealed positive correlation between GC12 and GC3 in DRGs and XMGs (Table 5). These results suggest that natural selection played a major role while mutation pressure played minor

role in shaping the composition of coding sequence of *K. pneumoniae* [25].

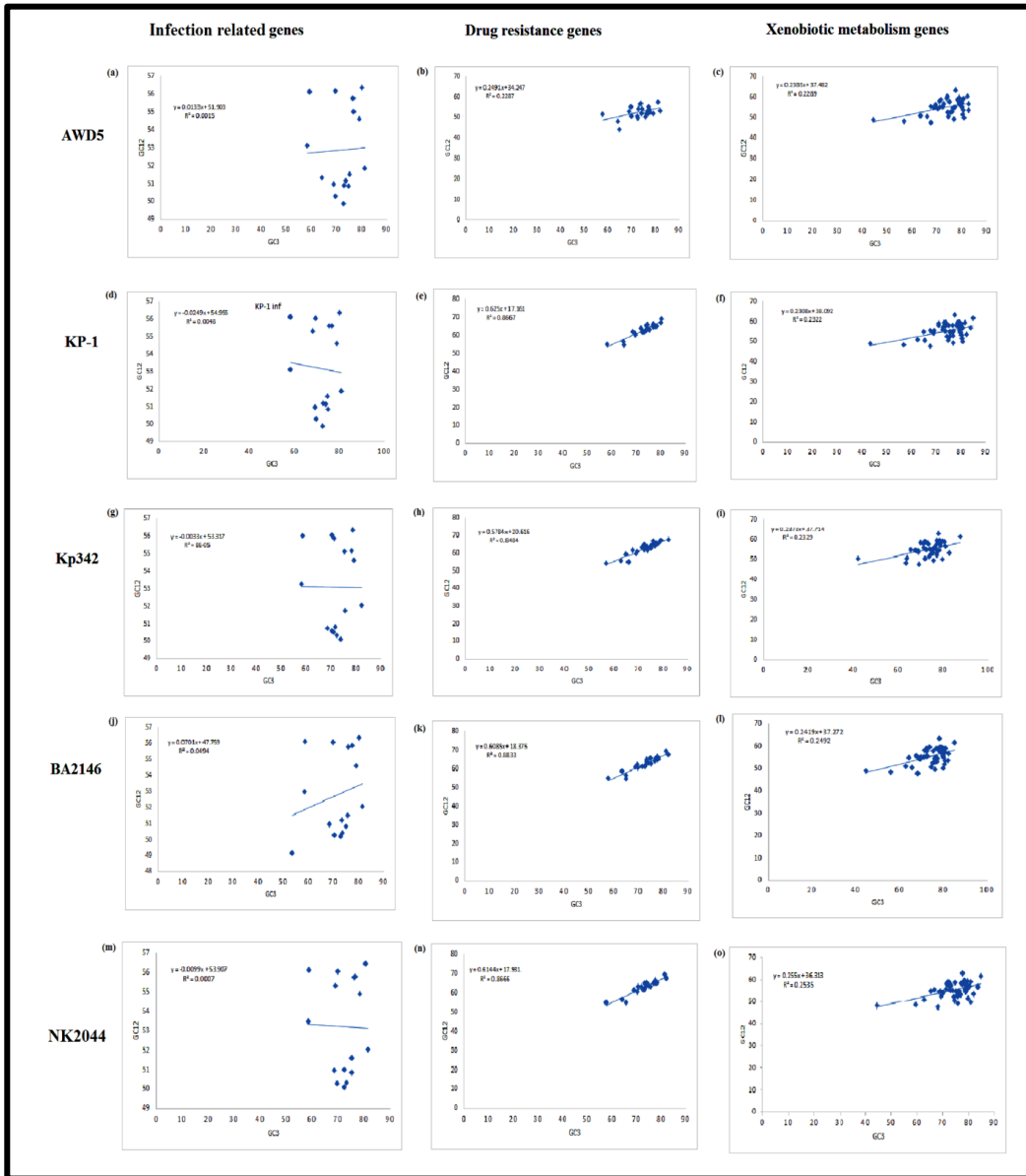


**Figure 7:** Neutrality plot of infection-related genes, drug resistance gene and xenobiotic metabolism genes of *K. pneumoniae* genome AWD5 (a-c), KP-1 (d-f), Kp342 (g-i), BA2146 (j-l), NK2044 (m-o). Individual genes are plotted based on the mean GC content in the first and second codon position (GC12) versus GC content of the third codon position (GC3).

**Conclusion:**

A comparative genome analysis shows that clinical and non-clinical strains of *K. pneumoniae* are similar and are not separated by phylogeny. However, gene level comparison help distinguish these isolates where *mdtABCD*, toxin-antitoxin systems are distinctive to clinical isolates and *catB*, *benA*, transporter genes for citrate utilization are limited to non-clinical isolates. Thus, these data help distinguish clinical and non-clinical isolates of *K. pneumoniae* towards the understanding of genome diversity during speciation.

**Supplementary Materials:**

The gene network of specific core genes of clinical and non-clinical isolates was analyzed in Cytoscape (Figure 5a & 5b). The gene network for the unique core genes of clinical isolates consisted of 64 nodes and 191 edges. The relationship of genes of interest in our study with functional partners was specified to find co-expression, genetic interactions, and physical interactions. A single cluster was identified. The relationship of the selected genes was correlated with other genes, for example, phosphoproteins that are assistant transporter of drug transmembrane transport (*baeS*, *baeR*, *uvrY*) correlated to multidrug efflux system (*mdtABCD*). These two clusters were further connected closely to uracil catabolism system. Similarly, gene cluster of type II toxin-antitoxin module was connected to a group of genes with the phosphotransferase system and fructose specific subsystem. Hierarchical clustering led to the removal of four outlier samples (*malE*, *aslA*, *yaiZ*, *ushA*), which belong to the unique core of clinical isolates. This is probably due to no interaction with the genes in the network.

We then expanded the analysis of the gene network for the unique core genes of non-clinical isolates that consisted of 36 nodes and 101 edges. Hierarchical clustering led to the removal of seven outlier samples (*arsB*, *benA*, *betB*, *catB*, *ppx*, *sufE*). Interestingly, two clusters were identified in which the cluster for the query gene *ppdA* with its functional partners showed no interaction with other query genes. In the larger cluster, the relationship of the genes of interest was also correlated, such as an integral component of plasma membrane *ynfA*; *melB* interacted with plasma membrane genes *ubiD*, *ybdJ* with its gene cluster. The query gene of citrate utilization (*citCDE*) showed its interaction with functional partners of the gene cluster along with other genes. As well, the functional partners of the outliers' *catB*, *benA*, and *arsB* were specified, which have a functional role in the catabolism of catechol, benzoate and arsenite transport. It was noted that the functional partners were not part of the core genome of the respective group; however, it surely had interactions, and hence influence the functions of these genes.

To understand the topological properties of these networks, the probability of the node degree distribution  $P(k)$  showed that each network satisfied scale-free topology following power law ( $r^2 > 0.6$ ; in core genes of clinical genomes and  $r^2 > 0.2$  in core genes of non-clinical genomes) (Figure 5c & d). The node distribution based on degree implied the presence of genes with centrality values. The distribution following the power law distribution and showing the nature of the scale-free network suggested a hierarchical organization in the network.

**References:**

- [1] Jones RN. *Clin Infect Dis* 2010 **51**:S81 [PMID: 20597676]
- [2] Matsen JM *et al.* 1974 *Appl. Microbiol* **28**: 672 [PMID: 4607526]
- [3] Lee KWK *et al.* *Genome Announc.* 2013 **6**: e1082 [doi: 10.1128/genomeA.01082-13]
- [4] Rajkumari J *et al.* *3 Biotech* 2018 **8** [doi.org/10.1007/s13205-018-1134-1]
- [5] Holt KE *et al.* *PNAS* 2015 **112**(27): E3574 [doi: 10.1073/pnas.1501049112]
- [6] Lefebure T *et al.* *Genome biology and evolution* 2010 **2**: 646 doi: 10.1093/gbe/evq048
- [7] Segerman B. *Frontiers in Cellular and Infection Microbiology* 2012 **2**(116) [doi: 10.3389/fcimb.2012.00116]
- [8] Runcharoen C *et al.* *Genome Medicine* 2017 **9** [doi: 10.1186/s13073-017-0397-1]
- [9] Bulmer M. *J. Evol. Biol.* 1988 **1**: 15 [doi.org/10.1046/j.1420-9101.1988.1010015.x]
- [10] Wright F. *Gene* 1990 **87**: 23 [doi: 10.1016/0378-1119(90)90491-9]
- [11] Babicki S *et al.* *Nucleic acids Res.* 2016 **44**:W147 [doi: 10.1093/nar/gkw419]
- [12] Montojo J *et al.* *F1000Research* 2014 **3** [PMID: 25254104]
- [13] Chen X *et al.* 2018 *Front. Microbiol.* **9**:1910 [doi: 10.3389/fmicb.2018.01910]
- [14] Kulsum U *et al.* 2018 *Adv Exp Med Biol.* **1052**:39 [doi: 10.1007/978-981-10-7572-8\_4]
- [15] Zhao Y *et al.* 2012 *Bioinformatics* **28**:416 [PMID: 22130594]
- [16] Zhao Y *et al.* 2018 *BMC Genomics* **36** [PMID: 29363431]
- [17] Caputo A *et al.* *Biology Direct* 2015 **10** [PMID: 26420254]
- [18] Fouts DE *et al.* *Plos Genetics* 2008 **4**:e1000141 [doi:10.1371/journal.pgen.1000141]
- [19] Chou HC *et al.* *Infection and Immunity* 2004 **72**:3783 [doi: 10.1128/IAI.72.7.3783-3792.2004]
- [20] Bialek-Davenet S *et al.* *Emerging Infectious Diseases* 2014 **20**: 1812 [doi.org/10.3201/eid2011.140206]
- [21] Podschun R. *Zentralbl Hyg Umweltmed* 1990 **189**: 527 [PMID: 2200423]

- [22] Zhang Z *et al. Plos one* 2013 **8**: e81469  
[doi.org/10.1371/journal.pone.0081469]
- [23] Chen Y. *Biomed. Res. Int.* 2013 **2013**:406342 [doi:  
10.1155/2013/406342]
- [24] Sueoka N. *Proc. Natl. Acad. Sci.* 1988 **85**:2653 [doi:  
10.1073/pnas.85.8.2653]
- [25] Chakraborty S *et al. Genomics* 2019 **111**:167  
[doi.org/10.1016/j.ygeno.2018.01.013]

**Edited by P Kanguane**

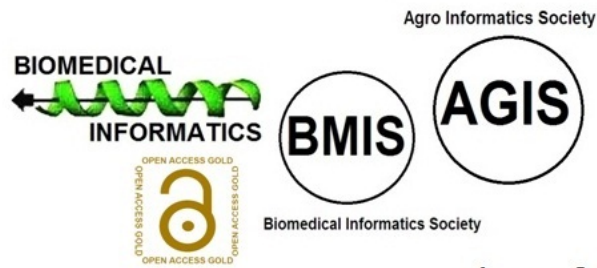
**Citation:** Rajkumari *et al.* *Bioinformation* 16(3): 256-268 (2020)

**License statement:** This is an Open Access article which permits unrestricted use, distribution, and reproduction in any medium, provided the original work is properly credited. This is distributed under the terms of the Creative Commons Attribution License

Articles published in BIOINFORMATION are open for relevant post publication comments and criticisms, which will be published immediately linking to the original article for FREE of cost without open access charges. Comments should be concise, coherent and critical in less than 1000 words.

# BIOINFORMATION

*Discovery at the interface of physical and biological sciences*



*since 2005*

# BIOINFORMATION

*Discovery at the interface of physical and biological sciences*

*indexed in*

